Partial volume-related errors in parameters derived from dynamic contrast-enhanced MRI – implications for clinical trials

A. Banerji[1], Y. Watson[1], C. Roberts[1], A. Caunce[1], G. A. Buonaccorsi[1], and G. J. Parker[1]

[1]Imaging Science and Biomedical Engineering, School of Cancer and Imaging Sciences, The University of Manchester, Manchester, Greater Manchester, United Kingdom

Introduction Tracer kinetic model parameters are frequently used in clinical trials to measure the efficacy of cancer therapeutics. Typically, the parameters are estimated for each voxel within a volume of interest (VOI) that is drawn around the tumour. The mean or median value is then calculated for the VOI and compared at different stages of the treatment. A simultaneous reduction in the tumour volume may also be observed. Voxels on the edge of the VOI are likely to include non-tumour tissue, and in this work we aim to investigate the influence of partial volume effects (PVEs) on the mean and median values as the tumour shrinks. This is of particular interest in the liver where the dual blood supply may lead to contrast agent concentration time courses that differ significantly from that of an arterial tumour rim. The liver is a common site of metastasis from colorectal cancer and there is also an increased incidence of hepatocellular carcinoma when cirrhosis is present. We use a software phantom generator[1] to synthesise tumour and liver data sets to provide controlled test data with which to evaluate the influence of partial volume effects.

Synthetic data generation The liver was modelled using a dual-input single-compartment model[2] with flow values from work by Van Beers[3] where the model was fitted to acquired dynamic contrast-enhanced (DCE) CT data. A population average was used for the arterial input function[4] and the portal input function was constructed by recreating the relationship seen to the shape of the AIF in published work[3]. The tumour was modelled using a single-input dual-compartment model[5] (the extended Kety model) with parameter values based on those found from fitting the model to previously acquired DCE-MR data. Zero mean Gaussian noise was added to the images with a standard deviation equivalent to a signal to noise ratio of 10 in the pre-contrast images. PVEs were emulated by defining tissue masks at twice the in-plane resolution and applying a Gaussian kernel with a width of three voxels. Spoiled gradient echo T_1 weighted images were generated with a 128x128x25 matrix and a voxel size of 3x3x8 mm.

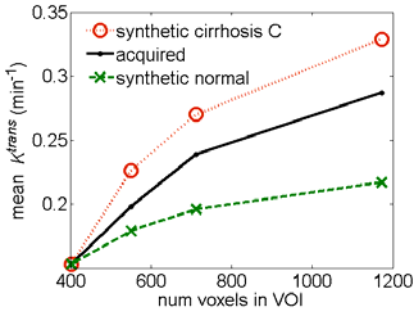

Fig. 1. Mean K^{trans} values for a tumour VOI in acquired data, in a synthetic liver with cirrhosis, and in a healthy synthetic liver. The tumour VOI is dilated three times by a voxel width as shown in Fig. 2.

Fig. 2. K^{trans} maps for a tumour VOI in acquired data (left) and the additional rings added for each of the three dilations.

Methods Firstly, K^{trans} values from the synthetic images were compared against an acquired data set. Mean K^{trans} values were calculated for a tumour VOI in the acquired data set. The VOI was then dilated in 3-D by a voxel width three times and the mean values for the three dilated VOIs calculated. The parameter maps for the tumour were then embedded in a synthetic liver with flow values corresponding to a healthy volunteer and also corresponding to cirrhosis Child-Pugh classification C[3]. The mean K^{trans} values were then measured for the same VOIs as for the acquired data. In a second experiment, synthetic data sets were generated to emulate a tumour that shrinks at subsequent visits in a clinical trial. Images were created with the tumour located in healthy liver tissue and in cirrhotic liver. To simplify implementation and to provide clarity regarding the magnitude of potential PVE-induced bias the simulated model parameters were left unchanged. K^{trans} mean and median values were compared for the different tumour sizes to the known ground truth. In all experiments K^{trans} was calculated by fitting the extended Kety model on a per voxel basis using locally written software and the VOIs were drawn by an experienced investigator.

Results Fitting the extended Kety Model to synthetic data generated using the Materne model gives a mean K^{trans} value of 0.42 min^{-1} for cirrhotic liver and 0.25 min^{-1} for normal liver. As the VOI of a tumour is dilated in the acquired data set the mean K^{trans} values increase from 0.15 min^{-1} to 0.29 min^{-1} (see Figs. 1 and 2). A similar effect is seen when the tumour in embedded in synthetic data with K^{trans} increasing to 0.22 min^{-1} for normal liver and 0.33 min^{-1} for cirrhotic liver. When emulating a reduction in tumour size, the median value is approximately 0.21 min^{-1} until the tumour VOI reduces to below approximately 80 voxels (see Fig. 3). At approximately 20 voxels the median has increased to 0.23 min^{-1} for a tumour in normal liver and 0.33 min^{-1} when in cirrhotic liver. (The ground truth for the tumour is 0.20 min^{-1}). The mean value for the tumour is at least 0.21 min^{-1} in normal tissue and at least 0.22 min^{-1} in cirrhotic tissue.

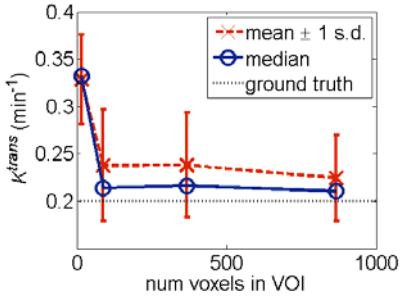

Fig. 3. Mean and median K^{trans} values for a VOI around a tumour whose ground truth K^{trans} value remains the same, but size decreases. The tumour is located in a liver with cirrhosis.

Conclusion When non-tumour liver tissue is present in a tumour rim voxel a higher apparent K^{trans} value is seen which can lead to overestimation of the mean and median K^{trans} values at smaller tumour sizes of about 20 voxels. This overestimation is greater when the tumour is located in a cirrhotic liver compared with healthy liver tissue. Above a size of approximately 70 voxels the median K^{trans} value reflects the ground truth and is more accurate than the mean. Our findings have implications for therapeutic trials of novel agents where treatment-induced changes in tumour size in the liver may lead to false conclusions regarding changes in microvascular function.

References **[1]** Banerji, A., et al. in Proc. ISMRM 16th meeting. 2008. **[2]** Materne, R., et al., Clin Sci (Lond), 2000. 99(6): p. 517-525. **[3]** Van Beers, B., et al., Am. J. Roentgenol., 2001. 176(3): p. 667-673. **[4]** Parker, G., et al., Magn. Reson. Med., 2006. 56(5): p. 993-1000. **[5]** Tofts, P., Journal of Magnetic Resonance Imaging, 1997. 7(1): p. 91-101.